

AN EVALUATION OF GALILEO - VIKING DIFFERENCED RANGE
IN GALILEO - MARS FLYBY NAVIGATION

F. B. Winn, E. W. Walsh, M. P. Ananda, F. T. Nicholson

Jet Propulsion Laboratory
California Institute of Technology

ABSTRACT

The navigational requirements of Galileo as it swings by Mars [flyby distance is 275 km from the Martian surface; 25 km (1σ)] are going to be met with interferometric angular measurements (VLBI) and range and range-rate measurements. Like VLBI, dual spacecraft differenced range is less sensitive to Mars ephemeris errors and tracking station location errors than conventional range and Doppler. Similarly, differenced range provides angular information about the separation between the Mars Viking Lander I and the Galileo spacecraft. In covariance studies, dual spacecraft range coupled with conventional range and Doppler is shown to estimate the Galileo-Mars flyby distance to better than 10 km (1σ) which is comparable to the VLBI performance. For the Galileo-Mars flyby, dual spacecraft differenced range promises to be an excellent backup to VLBI if the Mars Viking Lander remains operational.

This paper presents the results of one phase of research carried out at the Jet Propulsion Laboratory, California Institute of Technology, under Contract NAS7-100, sponsored by the National Aeronautics and Space Administration.

I. INTRODUCTION

Galileo, a NASA spacecraft to be launched in 1984 by the Space Shuttle/IUS launch vehicle, will travel from earth to a Mars flyby on an ultra fast trajectory: a flight time of less than 100 days. On such a high acceleration trajectory (Fig. 1), conventional Galileo radiometric tracking data, 2-way range and Doppler, can establish the heliocentric position of the probe to a standard deviation of 11 km.

The Mars ephemeris has an additional 40 km 'in-track' position uncertainty such that the Mars-Galileo relative position uncertainty exceeds 40 km (1 σ). It is essential to know the Mars-Galileo relative position to better than 25 km (1 σ). The closer Galileo can be flown past Mars, the smaller the Galileo rocket maneuver that will be required to send Galileo on to the Jupiter system (Fig. 2). The ΔV requirement of Galileo's rockets increases 40 m/s per 100 km increase in the flyby distance (Fig. 3). The Mars flyby is being used to provide a controlled acceleration to the Galileo spacecraft.

Deep space probes, such as Galileo, are tracked and navigated from earth. That is, a radio carrier is beamed to a distant space probe. The probe transponds the radio tone back to earth. The frequency difference between the earth transmitted and received signal is the Doppler shift - a measure of the spacecraft radial velocity. Modulation placed on the radio carrier is used to measure the light time separation between earth transmission to and reception from the spacecraft. These conventional radio metric data types, Doppler and range, measure in the radial direction only.

Jet Propulsion Laboratory

Because of topocentric parallax, at any instant of time the radial velocity of a probe is different at each terrestrial tracking station. This uniqueness of Galileo and Viking* range and range-rate, that is dependent on topocentric position, permits the determination of the relative Galileo-Viking angular separation.

In covariance studies, Galileo conventional range and Doppler could estimate the Galileo-Mars flyby distance to 40 km (σ) while a combination of doubly differenced range which exploits the relative topocentric parallax in conventional range and Doppler yields a standard deviation of less than 10 km and does so 25 days before Mars encounter (Fig. 4).

Galileo Project plans call for the Galileo spacecraft to flyby Mars 275 km ($\sigma_d = 25$ km) above the planet's surface (Ref. 1). To achieve this accurate flyby two new technological advances must be accomplished: one, the Mars ephemeris must be improved to better than 25 km (σ) and this effort is in progress; two, a wide-band Very Long Base Interferometry technology must be developed that will permit the Galileo spacecraft and Mars trajectories to be defined in a quasar inertial reference frame. This latter effort is underway also and offers not only a means to reduce the Galileo-Mars relative trajectory errors but VLBI cancels the preponderance of the Deep Space Station (DSS) location effects on orbit determination.

* The Viking Mars Lander I softly touched down on the Martian surface on July 4, 1976, and it still functions. It is expected to be operational in the Galileo era.

As circumstances are now, the current Mars Ephemeris and DSS locations uncertainties limit the Galileo-Mars relative navigation such that a $\sigma_d \leq 25$ km is not achievable with Galileo radiometric range and doppler alone. Galileo-Viking doubly differenced range provides a promising approach to Galileo's navigation objectives independent of an improved Mars ephemeris or a new VLBI technology. It does require the survival of the Viking Lander, however, in 1984.

II. DOUBLY DIFFERENCED RANGE DEFINITION

Figure 5 shows two Deep Space Station (DSS) tracking first one spacecraft and then the other. Thus, four range measurements are obtained and although the order of the range measurements taken in Figure 5 are DSS-1 to Viking, DSS-1 to Galileo, DSS-2 to Viking and DSS-2 to Galileo, the order is arbitrary.

With a restricted view to a single spacecraft, it is easy to show that the relative topocentric range (Fig. 6) involving 2 DSS is

$$\Delta\rho = \Delta Z \sin \delta + \Delta L \cos \delta$$

where

$$\Delta\rho = \rho_2 - \rho_1$$

ΔZ = north-south projection of the DSS baseline on that plane possessing the baseline and the spacecraft

ΔL = east-west projection of the baseline

or

$$\Delta L = \Delta\lambda \cos (\alpha - \text{LST})$$

with

$\Delta\lambda$ being a linear separation between the DSS in the earth equatorial plane

LST = local sidereal time at the λ of the baseline

$$\lambda = \left(\lambda_{DSS_1} + \lambda_{DSS_2} \right) / 2$$

Now if the relative range, $\Delta\rho$, from 2 spacecraft are combined in a second difference

$$\begin{aligned} \Delta^2\rho &= \Delta\rho_G - \Delta\rho_V && \left[\begin{array}{l} G \text{ signifies Galileo} \\ V \text{ signifies Viking} \end{array} \right] \\ \Delta^2\rho &= \Delta Z \left[\begin{array}{l} \cos \delta_G \Delta\delta \\ - \Delta\lambda \left[\begin{array}{l} \sin \alpha_G - LST \\ \cos \delta_G \Delta\alpha \\ + \cos (\alpha_G - LST) \sin \delta_G \Delta\delta \end{array} \right] \end{array} \right] \end{aligned} \quad (1)$$

$\Delta^2\rho$ is a function of the relative plane-of-sky coordinates of the two spacecraft and the baseline projection onto the plane-of-sky. It's sensitivity to the Mars ephemeris is less than that of $\Delta\rho$ or ρ .

$$\frac{\partial \Delta^2\rho}{\partial \sigma'(\text{state})} = \frac{\partial \Delta\rho_G}{\partial \sigma'(\text{state})} - \frac{\partial \Delta\rho_V}{\partial \sigma'(\text{state})}$$

but

$$\frac{\partial \Delta^2\rho}{\partial (\text{Galileo State})} = \frac{\partial \Delta\rho}{\partial (\text{Galileo State})}$$

Specifically, $\Delta^2\rho$ is 20% (2 months before Mars encounter) to 50% (at encounter) less sensitive to the Mars ephemeris error than $\Delta\rho_G$ as is shown by the RSS of $\Delta\rho$ and $\Delta^2\rho$ partials with respect to the heliocentric position of Mars (Fig. 7).

In Figure 7 there are three graphs, one for each baseline used in the study.

Jet Propulsion Laboratory

DSS43 is located in Woomera, Australia. DSS63 is located in Madrid, Spain, and DSS14 is at Goldstone, California. The DSS approximate spherical coordinates are tabulated in Table I.

Since the DSS are separated in longitude, from 94° to 154° , Mars is in view over each baseline at different times. The Viking Lander can only be ranged in the cool morning Martian hours and only ranged once per Martian day. Thus, as indicated in Figure 7, the Viking Lander can be ranged about 50% of the days that Galileo is in flight. Table II presents the 43 different occasions. Each baseline can range the Lander for 8 to 12 days repetitively.

Each baseline's performance is not only time dependent, but is also governed by the alignment of the baseline with respect to the Galileo-Mars angular separation at encounter (Eq 1). In essence, the Viking and the Galileo $\Delta\rho$ measurements provide information as to the direction of each spacecraft with respect to the baseline but only in the direction of the baseline. Orthogonal to the baseline there is no information. And, of course, when $\Delta\rho$ measurements are differenced to obtain $\Delta^2\rho$, $\Delta^2\rho$ defines the earth centered angular separation between the two spacecraft only in the baseline direction. Figure 8 shows the baseline orientations relative to the Mars-Galileo direction at encounter. The DSS43 - DSS63 baseline which is approximately 4° offset, yields the strongest information concerning the flyby distance while the DSS63 - DSS14 ($\sim 12^\circ$ offset) and the DSS14 - DSS43 ($\sim 60^\circ$ offset) baselines provide progressively less information.

Table III itemizes the theoretical error assessments of $\Delta^2\rho$ resulting from instrumentation and transmission media.* From Table III it is apparent

* Philip Callahan, Jet Propulsion Laboratory, private communication

that it is thermal noise [galactic background (6°K), receiver front end electronics ($6^\circ\text{-}11^\circ\text{K}$), antenna cable (3°K), transmission media (10°K), etc.] when subjected to high gain that dominates the $\Delta^2\rho$ error budget. A full 90% of the $\Delta^2\rho$ RSS noise is from this source. The result is that $\Delta^2\rho$ should have an RMS error of $\sim 2\text{ m}$ and 2m is the a priori standard deviation used in covariance study. Most of the systematic errors due to solar plasma, troposphere, ionosphere, DSS clock errors, spacecraft and station delays cancel. In addition, since tracking stations are used redundantly to track both Galileo and Viking, DSS longitude errors tend to cancel in the formation of $\Delta^2\rho$ (Fig. 9). DSS uncertainties in the other two coordinates are of little consequence since their effect upon $\Delta^2\rho$ is from one to two orders of magnitude smaller yet.

III. THE GALILEO-MARS FLYBY DISTANCE COVARIANCE STUDY

The covariance analysis performed in this paper allows a maximum likelihood estimated with gaussian errors on the observations. The assumed observations include two-way coherent Doppler data from the Galileo spacecraft using the three Deep Space Network stations continuously, one Doppler measurement every one hour, one range measurement from the Goldstone station every day and the available doubly differenced range measurements as shown in the Table II. Since the dynamic state parameters are non-linear functions of the measurements, the observation equations are linearized and the results obtained are based on a linear estimator. When a standard maximum likelihood estimator is constructed, the computed statistics based on data noise errors, do not reflect the effect of model errors in the solution. Thus the statistics must be adjusted to

account for these effects.

The measurement equation can be written in the form

$$\bar{z} = A\bar{x} + C\bar{p} + \bar{e}$$

where \bar{z} is the vector of measurements, \bar{x} the vector of estimated parameters, \bar{p} the vector of model parameters whose effects on the estimated parameters are to be investigated and \bar{e} the measurement errors. A weighted least squares estimator of $\hat{\bar{x}}$ can be obtained by (Bryson and Ho, 1969)

$$\hat{\bar{x}} = (A^T P^{-1} A)^{-1} A^T P^{-1} \bar{z}$$

with the assumption that \bar{p} is a random vector of zero mean with covariance P_c , $E(\bar{e}) = 0$, $\text{Cov}(\bar{e}) = P$ and $E(\bar{p}\bar{e}^T) = 0$ and the covariance of $\hat{\bar{x}}$ is given by

$$P_x^c = \text{Cov}(\hat{\bar{x}}) = P_x + P_x A^T P^{-1} C P_c C^T P^{-1} A P_x$$

where $P_x = (A^T P^{-1} A)^{-1}$ is the prior covariance matrix. The matrix P_x^c is known as the 'consider' covariance matrix and the matrix A and C are the partial derivatives of the measurements with respect to the estimated and the consider parameters. Both the Galileo orbital state and Mars ephemeris parameters are treated as estimated parameters, and the station locations, Viking lander locations and Mars mass are treated as 'considered' parameters. The a priori uncertainties of the parameters are given in Table IV.

In the model used to assess $\Delta^2 \rho$, the trajectory parameters of the Galileo probe was estimated in a manner that considered the uncertainties associated with the Mars Ephemeris, the DSS location set, the mass of Mars, the Viking Lander position (Table IV).

With this parameter set and the Galileo data set (Table V), the Galileo

heliocentric position can be estimated to 35 km (σ), Figure 10, and this uncertainty stems principally from DSS location uncertainties. The Galileo trajectory does not sense the gravitational effect of Mars until the last day before encounter. Galileo travels over a million kilometers on that last day.

Figure 10, the 'Standard Deviation of Galileo Heliocentric Position', shows σ_{ρ} in kilometers as a function of time in days from Mars encounter or when each simulated Galileo data arc stops. All estimates of σ_{ρ} involve data that starts 88 days before Mars encounter. Each estimate, following the E-85^d estimate, has an additional five days of data added to the solution. All of the standard deviation plots presented have this same format.

Galileo, Mars-centered, position estimates have a standard deviation equal to the RSS of Galileo's heliocentric position sigma and the Mars ephemeris position standard deviation (Fig. 11a).

Figure 11 not only exhibits the standard deviation of the Galileo flyby but shows the components of σ_d related to the Mars Ephemeris ($\sigma_d \mid \text{Mars Ephemeris}$), the DSS locations ($\sigma_d \mid \text{DSS Locations}$) and data noise ($\sigma_d \mid \text{data noise}$).

Since Galileo is over a million kilometers away from Mars at E-1^d, Galileo does not see Mars gravitationally until E-2^h and any effort to utilize Galileo tracking data to improve the Mars ephemeris fails. Hence, the ephemeris provides a near constant 40 plus kilometer component to $\sigma_d(\text{RSS})$.

As indicated in Figure 11, $\sigma_d \mid \text{DSS Locations}$ increases as the earth-probe distance increases. That is, DSS angular location uncertainty in an Euclidian solar system results in larger and larger spacecraft linear position uncertainty with increased topocentric range. However, if DSS coordinates were estimated,

instead of considered, this procedural artifact would disappear as in Fig. 2.

And lastly, in Figure 11, the data noise is shown to fall off with the square-root of the number of observations.

When these $\Delta^2\rho$ observations of Table II are added to the conventional Galileo data of Table V, the effects of the Mars ephemeris and the DSS location uncertainties are reduced. This should be expected since the RSS of the partials of the Mars position coordinates (Fig. 7) and the DSS coordinates (Fig. 9) with respect to $\Delta^2\rho$ are 2 to 10 times smaller than those with respect to $\Delta\rho$. That is, each $\Delta^2\rho$ observation is less sensitive to these error sources, but $\Delta^2\rho$ and $\Delta\rho$ possess the same sensitivity to the Galileo-Mars relative state. Figure 12 exhibits the ephemeris, DSS, and data noise contributions to σ_d . The data ensemble of $\Delta^2\rho$, conventional range and Doppler yields a $\sigma_d < 10$ km (σ) 25 days before Mars encounter. This is an improvement over conventional data reductions of four-fold. As can be seen in Figure 12, the correlated ephemeris and DSS locations uncertainties in each ρ observation cancel in the formation of $\Delta^2\rho$. As modeled, Mars ephemeris and DSS location uncertainties still dominate the standard deviation of the Galileo-Mars encounter distance estimate, however, their combined RSS contribution is less than 10 km (σ).

Jet Propulsion Laboratory

Summary

This covariance study shows that Galileo-Mars navigation is improved four-fold when dual station range from both Galileo and Viking are added to conventional Galileo tracking data and reduced. In essence, the Mars ephemeris and the tracking station uncertainties are differenced out of the new doubly differenced range data type, to a large extent, while little Galileo-Mars relative state information is lost. The information content of doubly differenced range is analogous to that of wideband very long baseline interferometry and promises to be an efficient backup the Galileo Project planned VLBI. Doubly differenced range coupled with conventional tracking data can be used to estimate Galileo-Mars flyby distance to better than 10 km (σ).

Reference

Project Galileo Navigation Requirements, PD 625-565, JPL 19 April 1979, JPL Internal Document.

TABLE I: Tracking Station Spherical Coordinates

DSS	Longitude	Latitude
43	149.0	35.3
63	355.8	-35.3
14	243.1	40.3

TABLE II: VIKING LANDER DIRECT LINK RANGING OPPORTUNITIES

for

GALILEO NAVIGATION, 1984

POINT	DSS BASELINE	DATE	POINT	DSS BASELINE	DATE
1	63-14	22 March 84	25	14-43	4 May 84
2	"	23 March 84	26	"	6 May 84
3	"	24 March 84	27	"	7 May 84
4	"	25 March 84	28	"	8 May 84
5	63-14	26 March 84	29	"	9 May 84
6	14-43	29 March 84	30	"	10 May 84
7	"	30 March 84	31	14-43	11 May 84
8	"	31 March 84	32	43-63	17 May 84
9	"	1 April 84	33	"	18 May 84
10	"	2 April 84	34	"	20 May 84
11	"	3 April 84	35	"	21 May 84
12	"	5 April 84	36	"	22 May 84
13	14-43	6 April 84	37	14-43	23 May 84
14	43-63	14 April 84	38	63-14	27 May 84
15	"	15 April 84	39	"	29 May 84
16	"	16 April 84	40	"	30 May 84
17	"	17 April 84	41	"	31 May 84
18	43-63	18 April 84	42	"	1 June 84
19	63-14	25 April 84	43	63-14	2 June 84
20	"	26 April 84			
21	"	27 April 84			
22	"	29 April 84			
23	"	30 April 84			
24	63-14	1 May 84			

DSS 14 (Goldstone, California)
 DSS 43 (Woomera, Australia)
 DSS 63 (Madrid, Spain)

TABLE III: Doubly Differenced NSR Error Budget

INSTRUMENTATION:

STATION CLOCK STABILITY (15 MIN)	4 CM
STATION DELAY CALIBRATION	--
SNR (THERMAL NOISE)	200 CM
WAVEFORM DISTORTION	88 CM
SPACECRAFT DELAY	28 CM

MEDIA:

TROPOSPHERE (25° ELEVATION)	20 CM
IONOSPHERE (25° ELEVATION)	6 CM
SOLAR WIND	15 CM

RSS 222 CM

ASSUMPTIONS:

VIKING LANDER - GALILEO SEPARATION $\sim 5^\circ$

DATA AT OPPOSITION ~ 0.7 AU

TWO STATIONS OBSERVE LANDER IN TURN APPROX. 15 MIN EACH

SAME TWO STATIONS OBSERVE GALILEO IN TURN APPROX. 15 MIN EACH

TABLE IV: Galileo-Viking Parameter Set

PARAMETERS	MODEL STATUS	A PRIORI
Galileo State	Estimated	$\sigma_x = \sigma_y = \sigma_z = 10^7$ km; $\sigma_{\dot{x}} = \sigma_{\dot{y}} = \sigma_{\dot{z}} = 100$ km/s
Mars State	Considered	$\sigma_{\text{radial}} = 10$ km; $\sigma_{\text{in track}} = 40$ km; $\sigma_{\text{out-of-plane}} = 70$ km
DSS Locations*	Considered	$\sigma_{\lambda} = 3.0$ m; $\sigma_{r_s} = 1.5$ m; $\sigma_{r_z} = 15.0$ m
Viking Lander Locations	Considered	$\sigma_x = 10.0$ m; $\sigma_y = 40.0$ m; $\sigma_z = 300.0$ m; $\sigma_x = \sigma_y = \sigma_z = 10^{-3}$ m/day
Mars GM	Considered	$\sigma = 0.1$ km ³ /Sec ²

* r_s = DSS distance from terrestrial spin-axis

r_z = DSS distance from earth equator plane

TABLE V: Schedule for Conventional Data

DATA TYPE	(σ)	RATE	DSS ACQUIRING
Galileo Doppler	1 mm/s	1 pt/hr	14, 43, 63
Galileo Range	1 km	1 pt/pass	14
Start: 6 March 1984 (E_{σ} - 88 days)		Stop: 2 June 1984 (E_{σ} - 20 min)	

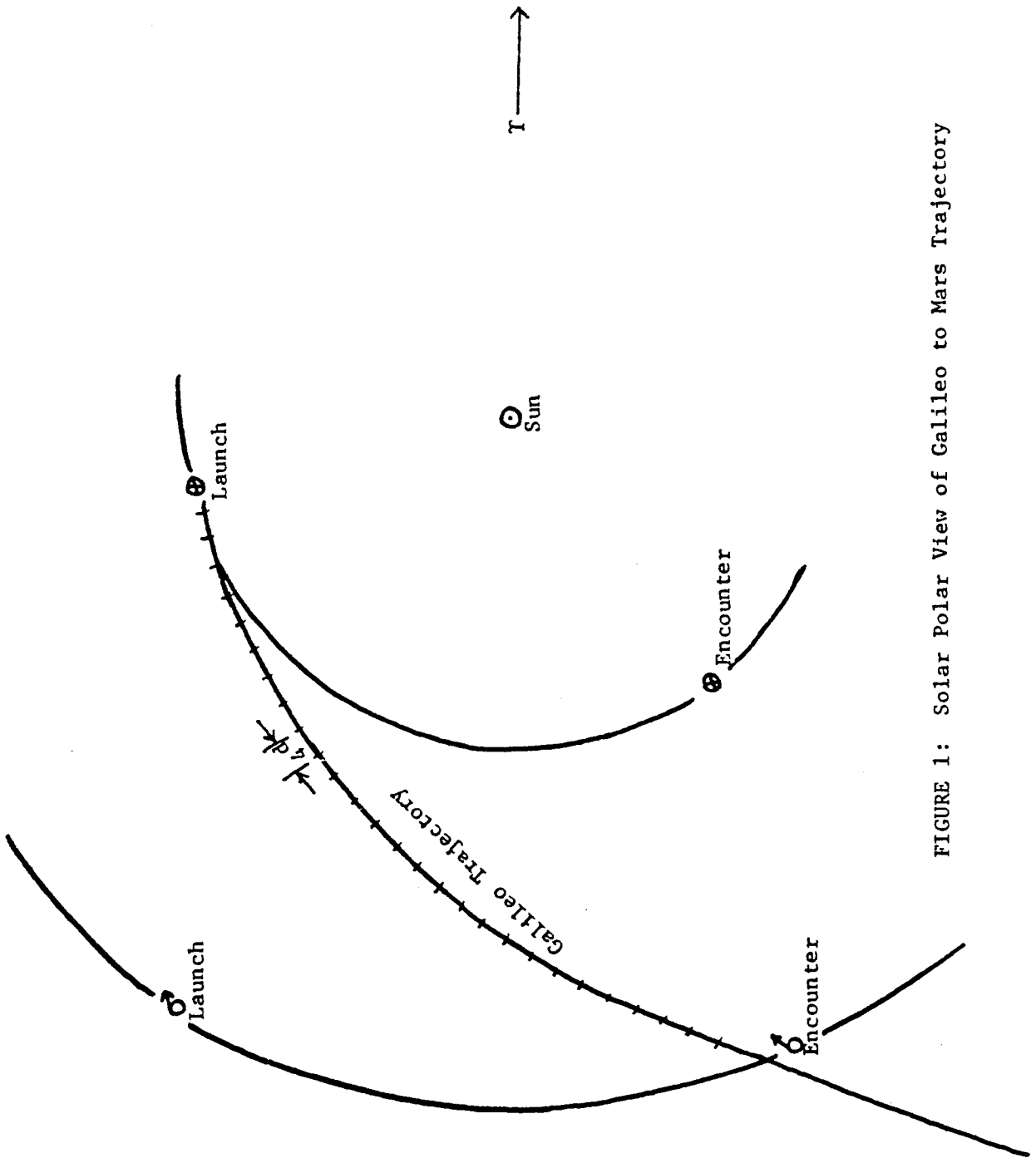


FIGURE 1: Solar Polar View of Galileo to Mars Trajectory

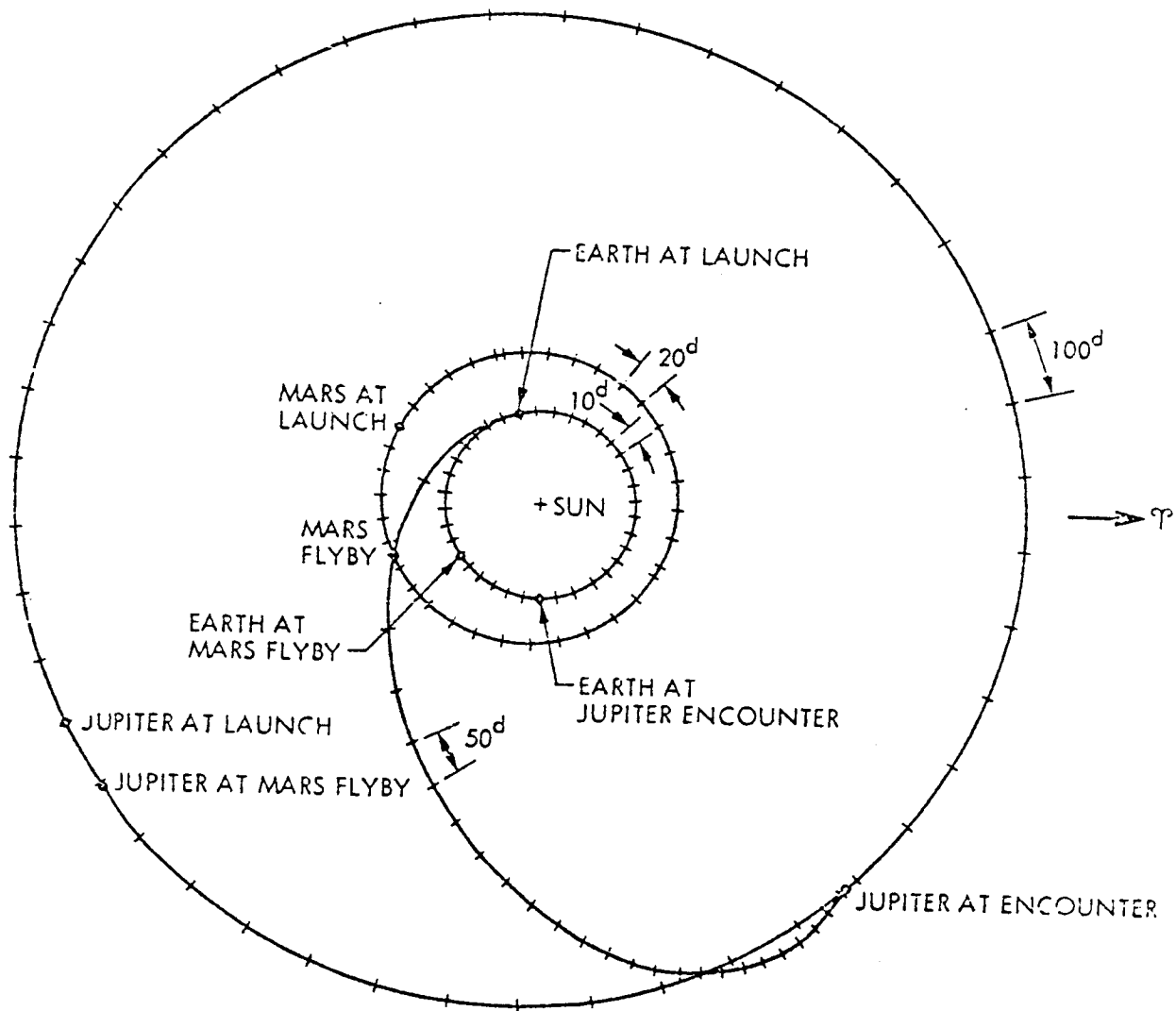


Figure 2 Heliocentric Ecliptic Pole View of Interplanetary Trajectory

FIGURE 3: ΔV and Flyby Distance Relationship

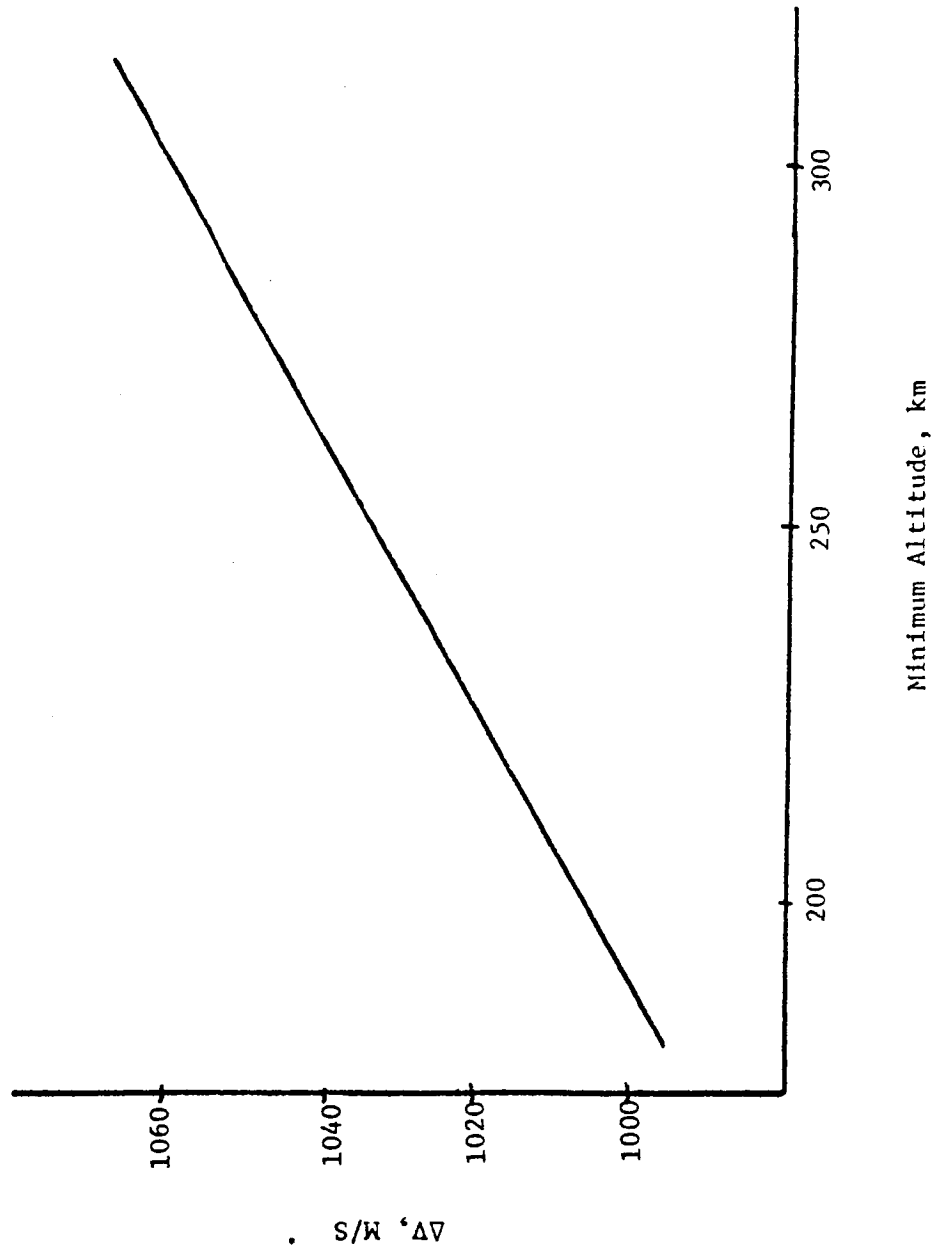
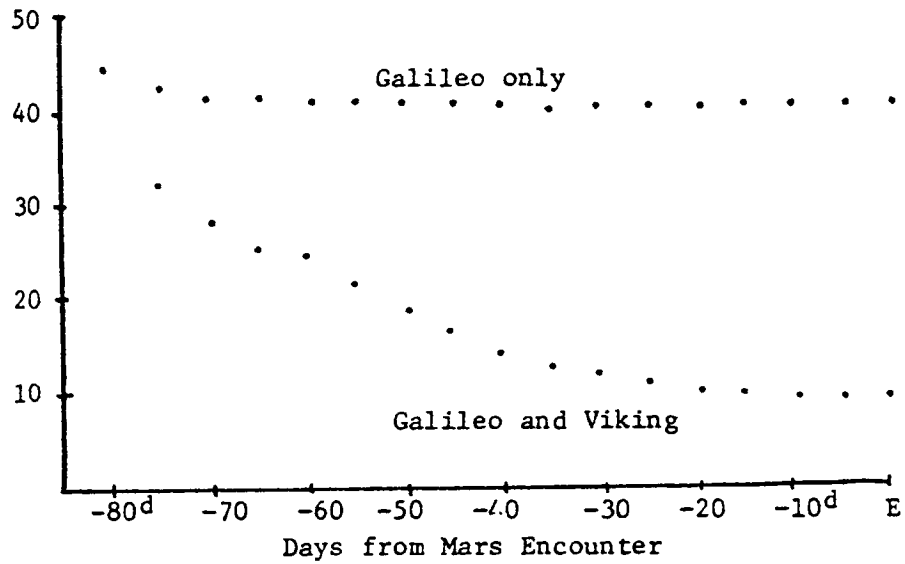


FIGURE 4: Uncertainty of Galileo-Mars Flyby Distance as a Function of Time-to-GO



First data occurs at E-88^d and continues uniformly until Mars encounter. Estimates of flyby distance are obtained every 5^d after E-85^d until Encounter.

FIGURE 5: Range Components of Doubly Differenced Range

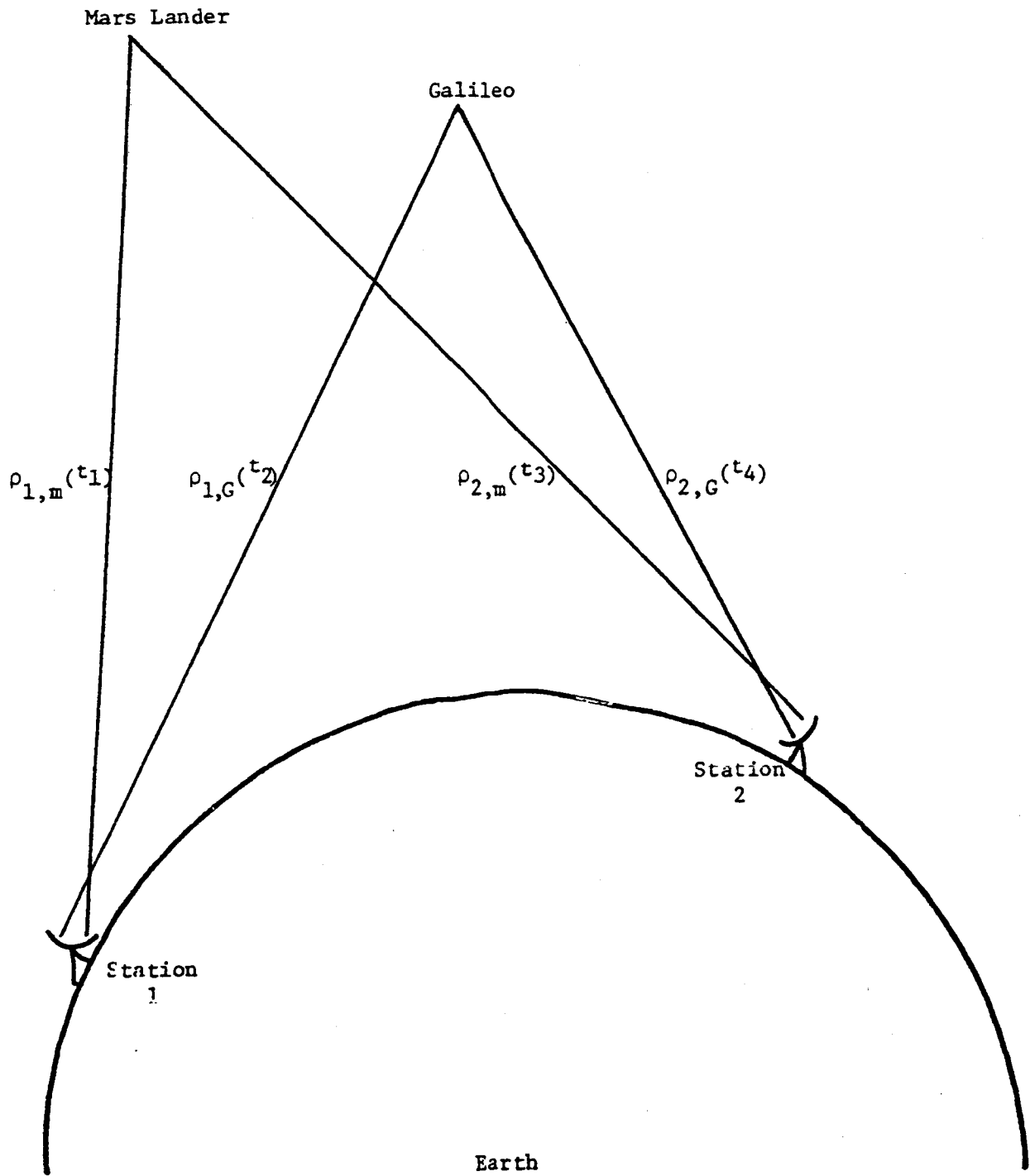
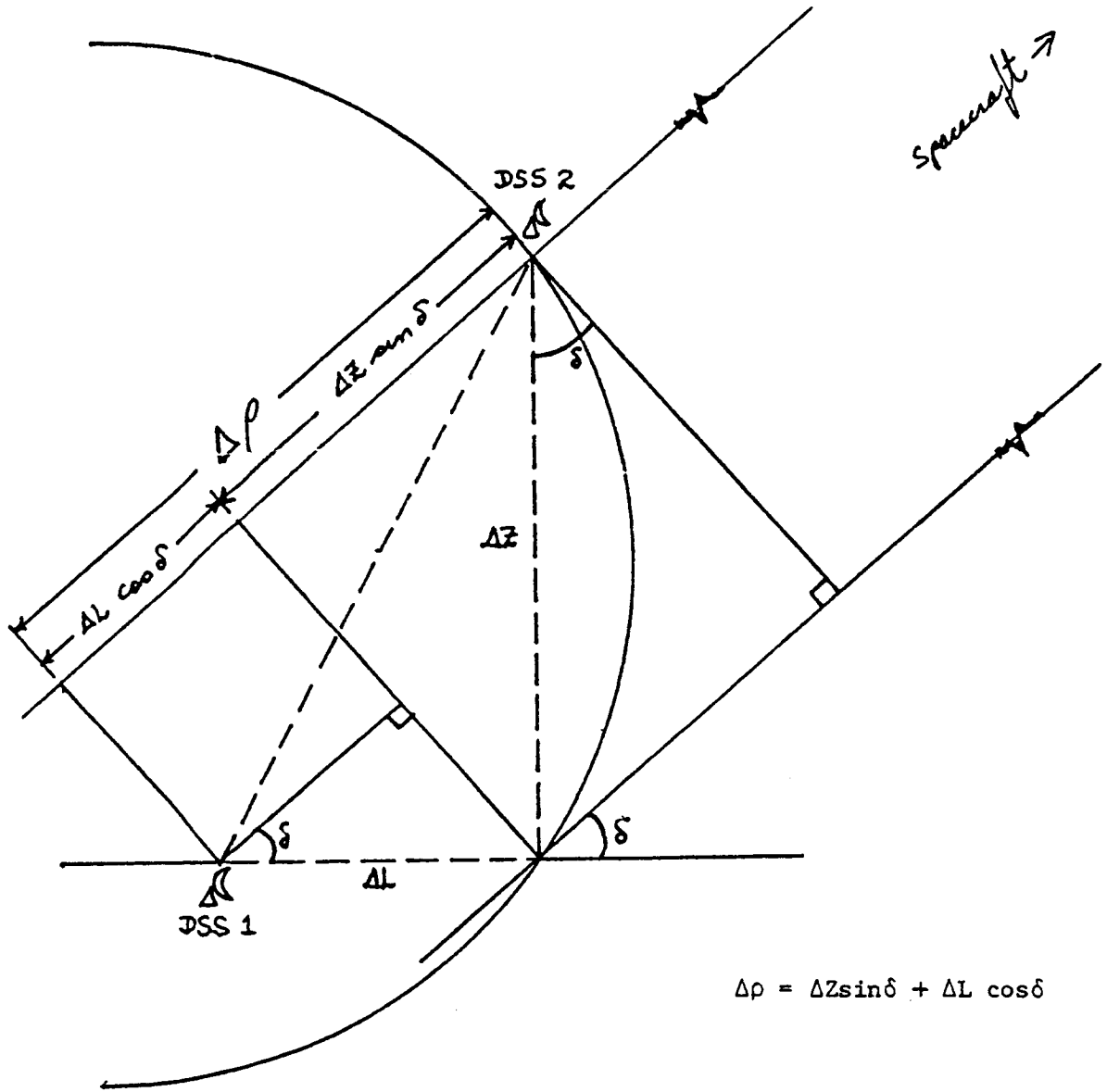


FIGURE 6: The Plane Geometry of Relative Range

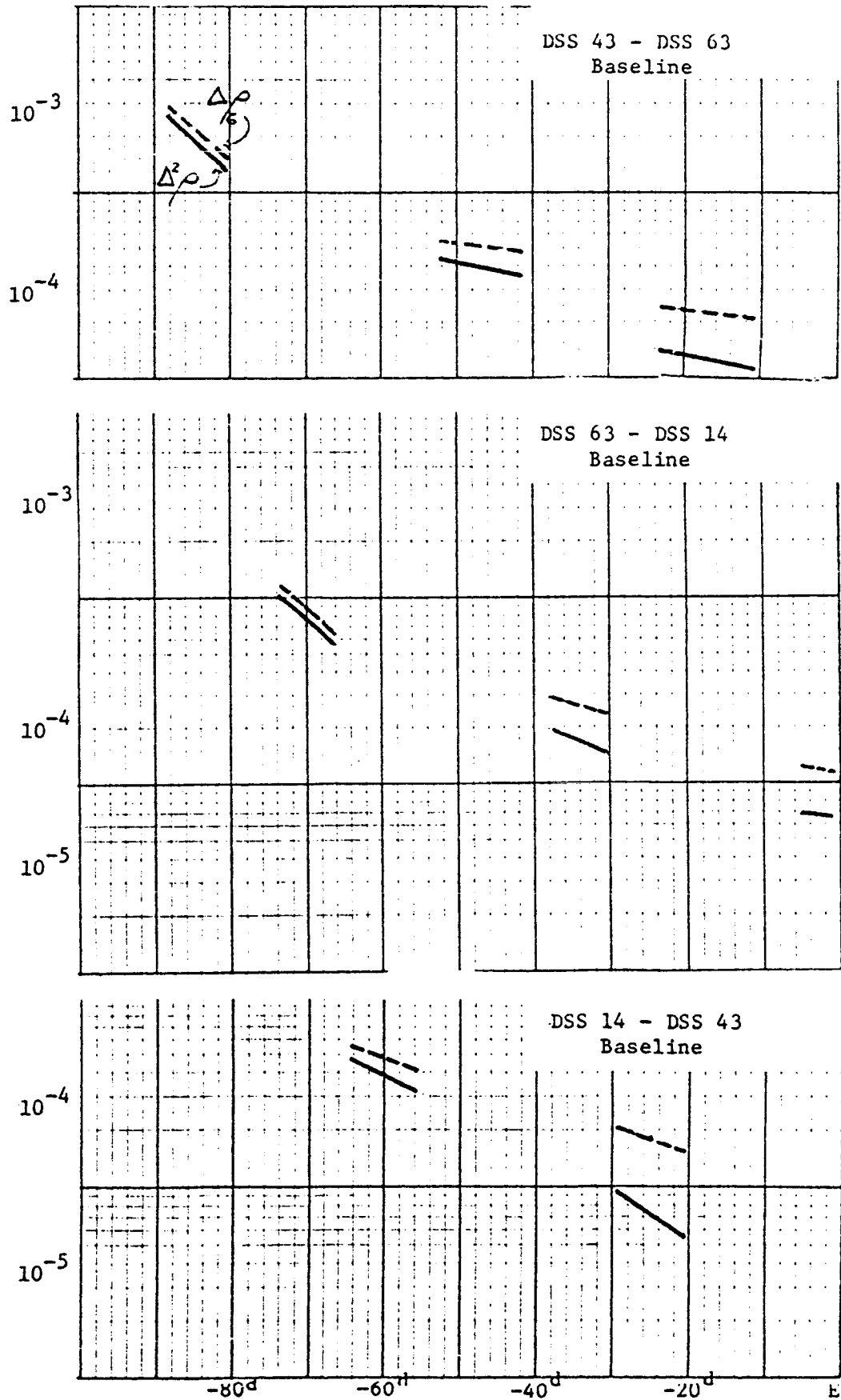


$$\Delta \rho = \Delta Z \sin \delta + \Delta L \cos \delta$$

DSS \equiv Deep Space Station of NASA's Deep Space Net

FIGURE 7: Sensitivity of $\Delta\rho$ and $\Delta^2\rho$ to Mars Position

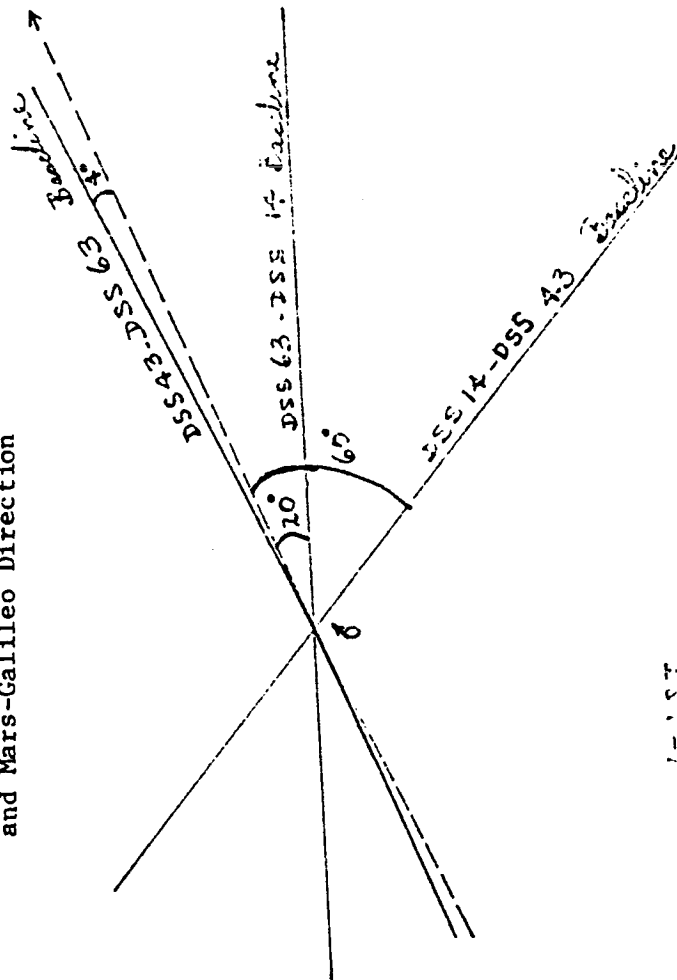
$$\left[\left(\frac{\partial \Delta^2 \rho}{\partial X \sigma'} \right)^2 + \left(\frac{\partial \Delta^2 \rho}{\partial Y \sigma'} \right)^2 + \left(\frac{\partial \Delta^2 \rho}{\partial Z \sigma'} \right)^2 \right]^{1/2} \text{ and } \left[\left(\frac{\partial \Delta \rho}{\partial X \sigma'} \right)^2 + \left(\frac{\partial \Delta \rho}{\partial Y \sigma'} \right)^2 + \left(\frac{\partial \Delta \rho}{\partial Z \sigma'} \right)^2 \right]^{1/2}, \text{ km/km}$$



Days from Mars Encounter

Galileo

FIGURE 8: Relative Orientation of Baselines and Mars-Galileo Direction



1348

FIGURE 9: Sensitivity of $\Delta\rho$ and $\Delta^2\rho$ to DSS Locations.

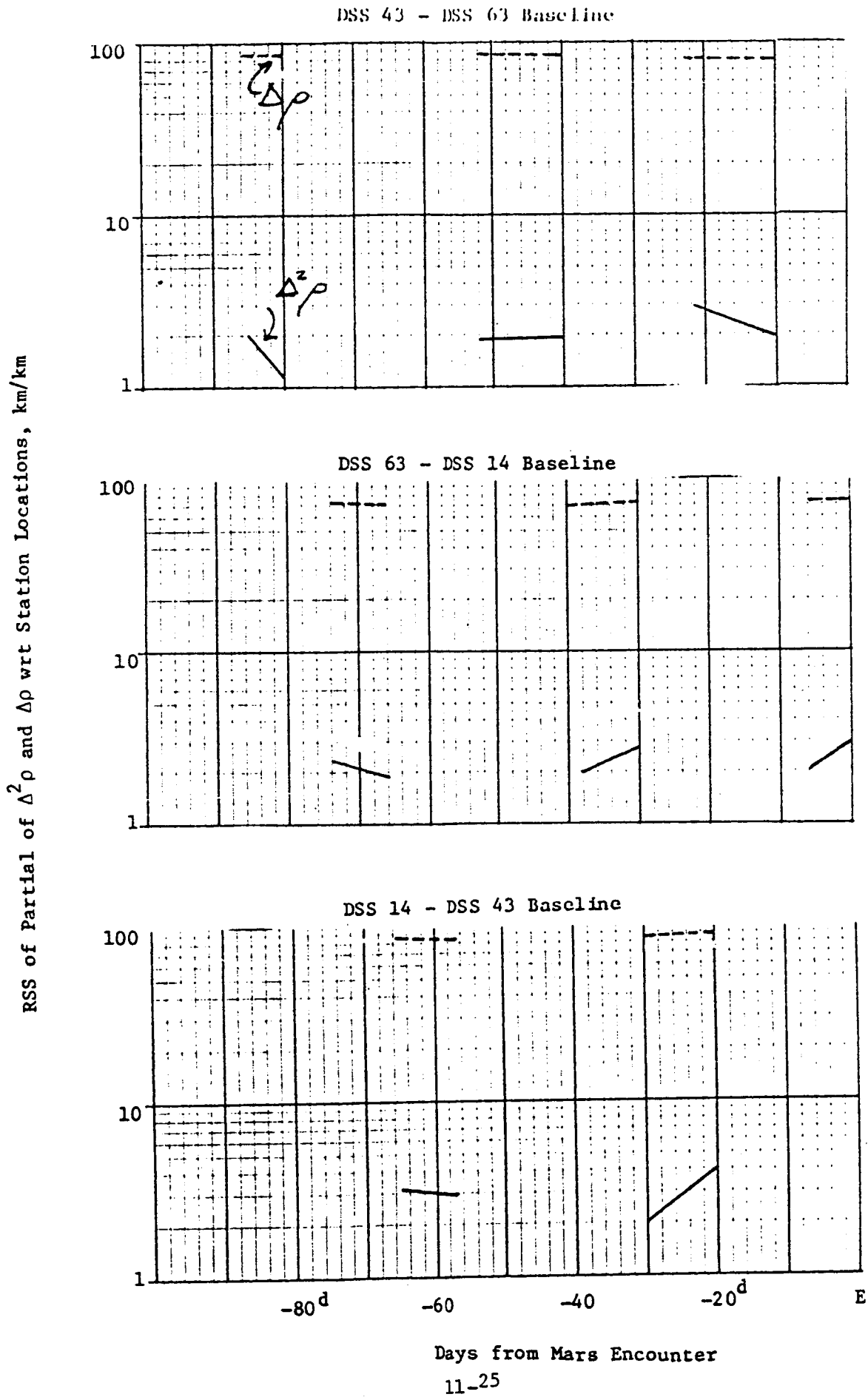


FIGURE 10: Standard Deviation of Galileo
Heliocentric Position Estimates, σ_p

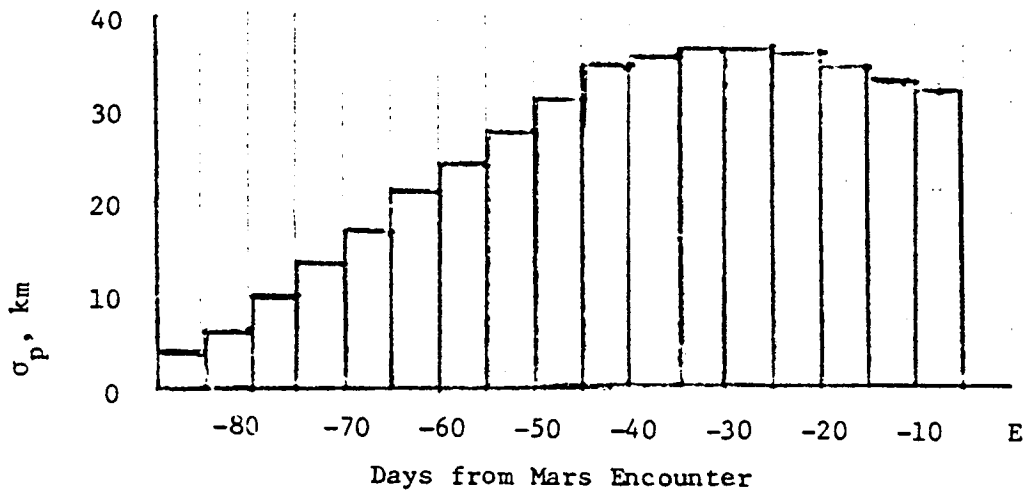


FIGURE 11: Standard Deviation of Galileo Flyby Distance From Mars
(Convention Galileo Tracking Data Only)

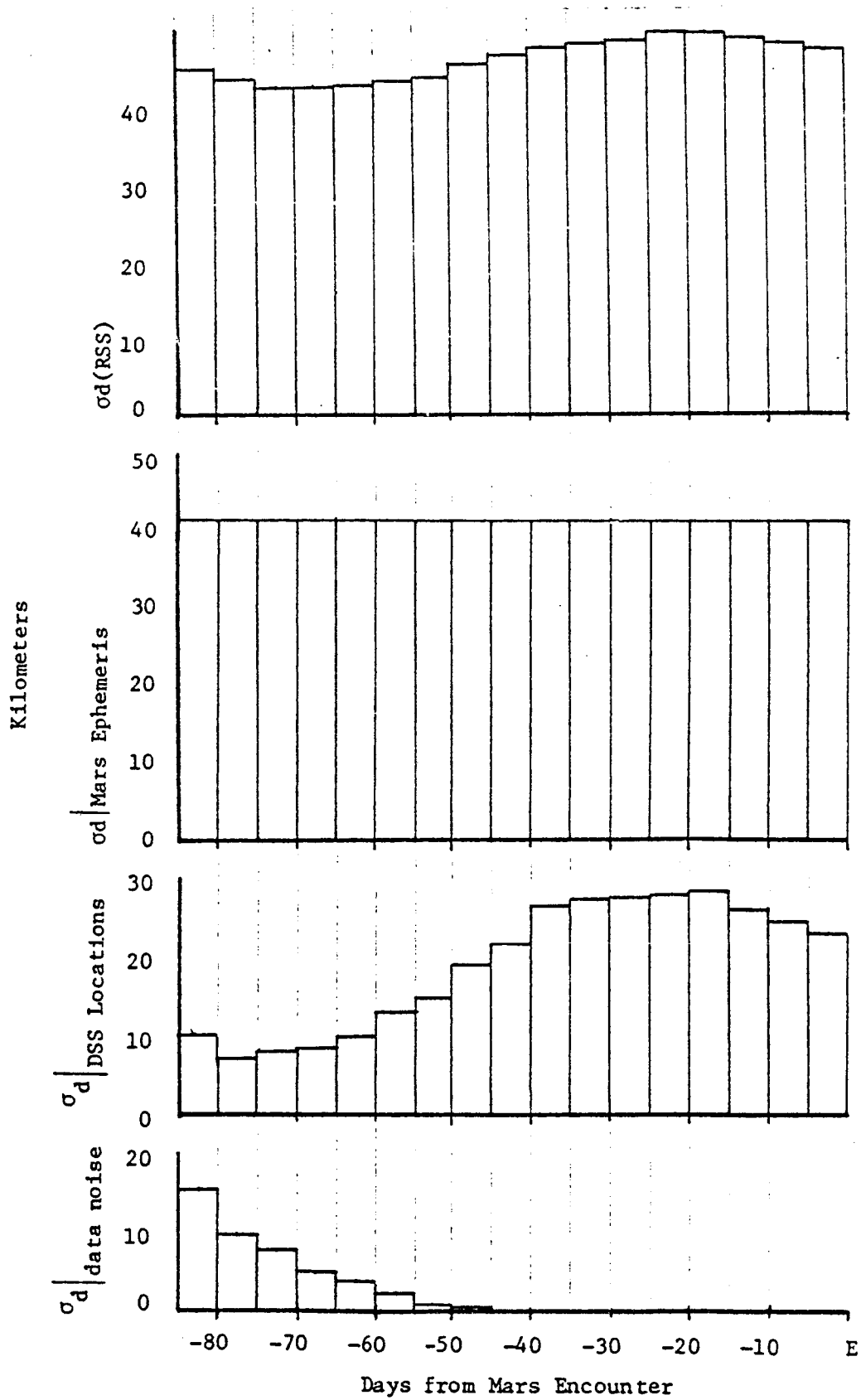


FIGURE 12: Standard Deviation of Galileo Flyby Distance from Mars (with Galileo-Viking $\Delta^2\rho$)

